Pharm Res (2012) 29:1832–1842
DOI 10.1007/s11095-012-0707-7

RESEARCH PAPER

Mass Spectrometry-Based Quantification of CYP Enzymes to Establish *In Vitro/In Vivo* Scaling Factors for Intestinal and Hepatic Metabolism in Beagle Dog

Aki T. Heikkinen • Arno Friedlein • Jens Lamerz • Peter Jakob • Paul Cutler • Stephen Fowler • Tara Williamson • Roberto Tolando • Thierry Lave • Neil Parrott

Received: 1 November 2011 / Accepted: 8 February 2012 / Published online: 22 February 2012

ABSTRACT

Purpose Physiologically based models, when verified in pre-clinical species, optimally predict human pharmacokinetics. However, modeling of intestinal metabolism has been a gap. To establish *in vitro/in vivo* scaling factors for metabolism, the expression and activity of CYP enzymes were characterized in the intestine and liver of beagle dog.

Methods Microsomal protein abundance in dog tissues was determined using testosterone-6β-hydroxylation and 7-hydroxycoumarin-glucuronidation as markers for microsomal protein recovery. Expressions of 7 CYP enzymes were estimated based on quantification of proteotypic tryptic peptides using multiple reaction monitoring mass spectrometry. CYP3A12 and CYP2B11 activity was evaluated using selective marker reactions.

Results The geometric mean of total microsomal protein was 51 mg/g in liver and 13 mg/cm in intestine, without significant differences between intestinal segments. CYP3A12, followed by CYP2B11, were the most abundant CYP enzymes in intestine. Abundance and activity were higher in liver than intestine and declined from small intestine to colon.

Conclusions CYP expression in dog liver and intestine was characterized, providing a basis for *in vitro/in vivo* scaling of intestinal and hepatic metabolism.

KEY WORDS beagle dog · CYP· intestinal metabolism · *in vitro/in vivo* scaling · MRM

ABBREVIATIONS

CYP	cytochrome P450
DIM	dog intestinal microsomes
DLM	dog liver microsomes
LCMS	liquid chromatography – mass spectrometry
MRM	multiple reaction monitoring
PBPK	physiologically based pharmacokinetics
PK	pharmacokinetics

INTRODUCTION

The Beagle dog is a commonly used pre-clinical species in drug research and development. It is utilized, for example, in preclinical safety testing, to screen clinical formulations and to explore the potential for pharmacokinetic food effects. Despite this utility, screening in the dog provides only a low throughput and results are often not directly translatable to human (1). In order to overcome these limitations and improve human

Electronic supplementary material The online version of this article (doi:10.1007/s11095-012-0707-7) contains supplementary material, which is available to authorized users.

A. T. Heikkinen • S. Fowler • T. Lave • N. Parrott (✉)
Non-Clinical Safety, Pharmaceuticals Division
F. Hoffmann-La Roche Ltd.
Grenzacherstrasse 124, B70/R130
CH-4070 Basel, Switzerland
e-mail: neil_john.parrott@roche.com

A. Friedlein • J. Lamerz • P. Jakob • P. Cutler
Translational Research Sciences, Pharmaceuticals
Division F. Hoffmann-La Roche Ltd.
Basel, Switzerland

T. Williamson
Celsis *In Vitro* Technologies
Baltimore, Maryland, USA

R. Tolando
Celsis *In Vitro* Technologies GmbH
Neuss, Germany

absorption predictions a physiologically based pharmacokinetic (PBPK) modeling approach using the dog to verify model assumptions was recently proposed (1,2). A weakness in this strategy is related to intestinal metabolism. The gut wall, in addition to the liver, is recognized as a site of significant first pass metabolism (3,4), but validated methods to incorporate intestinal metabolism into physiological models, especially for the beagle dog, are lacking.

The tools required for incorporating intestinal metabolism into physiological models can be broken down into three components: 1) a biochemically relevant *in vitro* system to characterize quantitatively the metabolic interaction between the compound of interest and the metabolic enzymes present in the gut wall; 2) *in vitro/in vivo* scaling factor(s) to scale the *in vitro* observed metabolism to the intact tissue (in practice, the abundance of enzymes *in vitro* and *in vivo* is used as the surrogate for scaling metabolic activity); 3) a physiological whole body model integrating metabolism with other mechanisms affecting pharmacokinetics (PK) and simulating the exposure of the compound to metabolic enzymes.

Several recombinantly expressed cytochrome P450 (CYP) enzymes (5) and microsomal preparations, potentially applicable for *in vitro/in vivo* scaling of intestinal and hepatic metabolism in beagle dog, are currently commercially available. Additionally, PBPK models for simulating beagle dog PK and in which the contribution of intestinal metabolism could be integrated have been published (2). However, the abundance of total microsomal protein and more specifically the expression of metabolic enzymes along the beagle dog intestine are currently not known in sufficient detail to be used as the basis for quantitative *in vitro/in vivo* scaling. In order to address this gap, this study focused on establishing the expression levels of metabolizing enzymes in the dog intestine and liver. The abundance of total microsomal protein in the beagle dog liver and along the intestine, and the abundance of several CYP enzymes in intestinal and liver microsomes were characterized. These data form the basis for *in vitro/in vivo* scaling of intestinal and hepatic metabolism using PBPK modeling in the beagle dog and the results of such modeling will be the subject of a future paper.

MATERIALS AND METHODS

Chemicals

Unless otherwise noted, all chemicals were obtained from commercial sources and were of analytical grade or better.

Preparation of Liver and Intestinal Microsomes

Beagle dog intestines and livers were extracted by Covance (Cumberland, VA) according to IACUC standards. Two male and two female beagle dog donors were utilized, ranging in age from 6 months to 13 months with a weight range of 7.8 kg to 13.7 kg. Briefly, animals were euthanized by intravenous injection of a barbiturate/phenytoin solution, and the livers and intestines were flushed with ice cold Viaspan (Barr Laboratories, Pomona, NY) before being surgically removed. The tissues were shipped in cold Viaspan on wet ice to Celsis *In Vitro* Technologies.

Intestinal enterocyte microsomes were prepared by Celsis *In Vitro* Technologies using a modification of the methods from Fasco *et al.,* (6) and Zhang *et al.* (7). Exact and fast distinction of the anatomical segments of small intestine based on visual inspection is challenging. Therefore, to minimize the tissue handling times and protein degradation during the process, the small intestine was divided into 6 equal length segments (mean 57 cm) designated as SI1 to SI6. Anatomically SI1 consists of the duodenum (~25 cm) and part the proximal jejunum and S6 consists of part of the distal jejunum and the ileum (~10 cm). Segments SI2-SI5 originate anatomically from the jejunum. The cecum (mean 6 cm) and colon (mean 34 cm) were collected as anatomical segments. Each segment was clamped at one end and filled with Wash Buffer (PBS, 40 ug/mL phenyl methyl sulphonyl fluoride (PMSF)). The other end was clamped to hold the buffer and the segments were gently agitated at 4°C for 5 min. Wash Buffer was drained out and the enterocytes were eluted by filling each segment with Elution Buffer (PBS, 1.5 mM EDTA, 0.2 mM PMSF, 0.5 mM DTT). The segments were placed in a plastic container filled with PBS and 20% (v/v) glycerol and shaken vigorously for 5 min at 4°C. The solution was drained from each of the eight segments into separate containers. The individual segments were refilled with fresh Elution Buffer and shaken for an additional 15 minutes. This elution process was repeated three times and the elutions from each segment were combined to create eight separate containers of pooled enterocytes. The cell suspensions were centrifuged at 2000×g for 10 min at 4°C. The supernatant was removed and the cell pellets were weighed before mixing with Enterocyte Homogenizing buffer (250 mM sucrose dissolved in dionized water, 0.2 mM PMSF) at a 3:1 buffer to tissue ratio. The cell pellets were homogenized thoroughly using three 15–20 s bursts of a medium Polytron (Kinematica, Lucerne, Switzerland) homogenizing tip at 9000 rpm. The homogenized suspension was centrifuged by Sorvall RC2-B (Thermo Scientific, Waltham, MA) at 9500×g for 20 min at 4°C. The supernatant from this spin (S9 fraction) was ultracentrifuged at 100,000×g for 44 minutes at 4°C to collect the microsomal pellet. The microsome pellet was resuspended in

250 mM sucrose dissolved in deionized water and the protein concentration was determined using Pierce BCA Assay *versus* bovine serum albumin (BSA) standard curve. Microsomes were immediately stored at −80°C.

Liver microsomes were prepared by mixing fresh liver tissue with Liver Homogenizing Buffer (5.3 mM Tris, 2 mM EDTA, 44.7 mM Trizma HCl, 150 mM KCl, supplemented with 20 mM 6-Di-tert-butyl-4-methylphenol) at a 3:1 buffer to tissue ratio. The liver tissue was mixed in a laboratory blender (Waring, New Hartford, CT) for 40 s at setting 6, transferred to a plastic beaker then thoroughly homogenized using three 15–20 s burst of a Polytron set at 9000 rpm. The homogenate was centrifuged at 9500×g for 20 min at 4°C and the S9 supernatant fraction was collected. The S9 supernatant was centrifuged at 100,000×g for 44 min at 4°C to yield the microsomal pellet. The pellet was resuspended in 250 mM sucrose dissolved in deionized water and protein concentration was quantified colormetrically using Pierce BCA Assay *versus* BSA standard curve. Microsomes were immediately stored at −80°C.

Determination of Microsomal Scaling Factors for Liver and Intestine

It is assumed there is no significant loss of metabolically relevant microsomal proteins present in the tissues during the enterocyte elution and the cell homogenization steps. The enterocytes lining the intestinal villi are believed to contain the majority of the drug metabolizing enzymes, such as CYP3A, present in the gut wall (8). This layer of cells is detached during the early phase of the elution process, whereas the crypt epithelium and the lamina propria are more resistant to elution with EDTA (6,7). Consequently, it is reasonable to assume that the eluted enterocyte fraction consists mainly of metabolically relevant intestinal cells and that the majority of metabolic enzymes present in the gut wall are preserved within the eluted enterocytes.

In contrast, there is a substantial loss of microsomal protein during the cell fractionation (9,10) and to correct for such losses recovery needs to be established with a suitable microsomal marker. The most commonly applied approach is to use total CYP content, quantified spectrally based on method by Omura and Sato (11), as the microsomal marker to correct for losses during cell fractionation (12) when estimating the amount of hepatic microsomal protein. However, due to insufficient sensitivity, this approach has limited utility in tissues with low CYP abundance, such as intestine. Consequently, more sensitive microsomal markers, testosterone-6β-hydroxylation, a marker of CYP3A12 activity (13) and 7-hydroxycoumarin (7-HC) -glucuronidation, mediated by unidentified UGT enzyme(s), were used in this study. The amount of microsomal protein (MP) in intact tissue (as mg/g tissue or mg/cm tissue) was estimated using the average recovery of two markers to correct for losses during cell fractionation (Eqs. 1 and 2):

$$\text{Fraction recovered} = (\text{Marker}_M * \text{MP}_{\text{Yield}})/(\text{Marker}_H * \text{HP}_{\text{Yield}}) \quad (1)$$

$$\text{MP} = \text{MP}_{\text{Yield}}/\text{Fraction recovered} \quad (2)$$

Marker_M and Marker_H refer to microsomal marker (metabolite formation rate as pmol/mg protein in this study) measured in microsomes and homogenate, respectively. MP_{Yield} and HP_{Yield} are the uncorrected yields of microsomal and homogenate protein respectively (as mg/g tissue or mg/cm tissue).

Enzyme Activity

Testosterone-6β-hydroxylation and 7-HC-glucuronidation were measured both in microsomes and in corresponding batches of enterocyte or liver homogenate. These reactions were used as the microsomal markers to correct for losses of microsomal protein during cell fractionation. The cofactors used consisted of an NADPH-regenerating system (NRS) for CYP activity or UDPGA for UGT activity. NRS contained 2.22 mM ß-NADP, 27.6 mM glucose-6-phosphate and 6 U/μL glucose-6-phosphate dehydrogenase in 2% (w/v) sodium bicarbonate solution. For glucuronide conjugation, UDPGA stock was diluted to 30 mM in 2% (w/v) sodium bicarbonate solution. The reaction buffer contained 0.3 mg/mL (intestinal samples) or 0.5 mg/mL (liver samples) of microsomal or homogenate protein and 600 μM (intestinal samples) or 500 μM (liver samples) testosterone or 30 μM 7-HC (both intestinal and liver samples) in 100 mM Tris buffer, pH 7.4. Reaction buffer was warmed to 37°C and reaction was initiated with NRS (1:3 dilution) for testosterone or UDPGA (1:20 dilution) for 7-HC and incubated at 37°C for 20 min. The reactions were stopped by adding an equal volume of methanol. Samples were stored at −70°C prior to bioanalytical analysis. The metabolites were quantified using UPLC/MS/MS or HPLC methods.

Diazepam N-demethylation to nordiazepam and 3-hydroxylation to temazepam were used as marker reactions for CYP2B11 and CYP3A12 activities, respectively. These reactions have been reported to be selective for these enzymes (13) and similar results were obtained also in preliminary experiments of this study (selectivity data is presented and further discussed in Supplementary Material). Incubations were performed at 37°C in 100 mM potassium phosphate buffer, pH 7.4, containing either dog intestinal or liver microsomes. The incubation times and enzyme concentrations were adjusted to ensure the linearity of

metabolic reactions. With the conditions used the formation of secondary metabolite oxazepam was negligible. The final protein concentration in all diazepam incubations was 0.25 mg/ml. In all incubations the final concentration of organic solvent (DMSO) was set to 0.5%. After 5 min pre-incubation, the reactions were initiated by addition of 1 mM NADPH and the reactions were stopped by adding an equal volume of ice cold acetonitrile. The metabolites formed were quantified by HPLC coupled with UV detection at λ=254 nm.

Total P450 was measured in liver microsomes using the carbon monoxide (CO) difference spectroscopy method modified from Omura and Sato (11). Immediately prior to performing the analysis, a P450 assay buffer was prepared containing 100 mM sodium dithionite in 0.1 M sodium phosphate (pH 7.4) with 20% (w/v) glycerol. The assay buffer was mixed thoroughly and stored on ice. Microsomes were thawed and diluted into P450 assay buffer at between 1 and 2 mg/mL of microsomal protein. The samples were vortexed and 1 mL of diluted microsomes was added to each cuvette of a Cary 3E spectrophotometer (Agilent, Santa Clara, CA). A reference scan was performed and the sample cuvette was gassed with CO for 30 s, with a flow rate of approximately one bubble per second. The total P450 concentration was calculated and the value was normalized using actual protein concentrations for each sample.

Quantification of CYP Enzymes

Denaturation and Digestion of Dog Microsome Samples for MRM

Sample preparation was carried out by combining protocols from (14,15). In brief, 25 µl dog microsome samples were denatured with trifluoroethanol, reduced and alkylated and then digested with trypsin. Resulting peptides were desalted by using Oasis HLB solid phase extraction columns (Waters). Eluates were evaporated in a centrifugal vacuum concentrator to dryness and stored at −80°C until reconstitution.

Liquid Chromatography-Mass Spectrometry

LC-MS analyses were performed on an Agilent 1100 series HPLC instrument comprising a binary capillary pump, a column compartment and a Micro-WPS auto sampler (tray at 4°C) coupled to a 4000 QTRAP LC/MS/MS system hybrid triple quadrupole/linear ion trap mass spectrometer (Applied Biosystems/MDS Analytical Technologies, Foster City, CA) equipped with a Turbo V ion source. Instrument control, data acquisition, and processing were performed using Analyst 1.5 software. The LC separation was performed on an Atlantis T3 C18 column (1.0 mm × 150 mm, particle size 3.0μm) from Waters (Milford, MA). Elution was performed at a flow rate of 60μL/min with 2% acetonitrile containing 0.1% (v/v) formic acid as eluent A and 98% acetonitrile containing 0.1% (v/v) formic acid as eluent B, employing a short linear gradient from 2% B to 15% B in 1 min. following a linear gradient from 15% B to 35% B in 20 min. The injection duty cycle was 28 min. taking into account the column equilibration time.

Peptide Selection

To develop a method for the quantification of CYP proteins, aliquots of dog intestinal and liver microsomes were reduced, S-carboxyamidomethylated and digested with trypsin. The resulting peptides were separated by capillary reversed phase HPLC and then analyzed using the MIDAS™ (MRM Initiated Detection And Sequencing) workflow (16), a process to find optimal MRMs on a 4000 QTRAP system (Applied Biosystems/MDS Sciex). The aim of this multiplex assay for protein targets from a subset of the highly homologous CYP dog proteins was to identify those few peptides possessing unique "transitions", i.e. transitions that allow unambiguous target identification and quantitation. The sequences of peptides selected for quantification of 7 CYP enzymes are presented in Table I.

Table I The Proteotypic Peptides Selected for Quantification of Beagle Dog CYP Enzymes in Intestinal and Liver Microsomes

Enzyme	Peptide sequence
CYP1A2	EAEALLSR
	SVQDITGALLK
	FLTADGTTINK
CYP2B11	EALVDNAEAFSGR
	QVYNNLQEIK
	NLIDTALSLFFAGTETTSTTLR
	DFIDAYLIR
CYP2C21	DFIDYFLIK
	FSLTVLR
	YGLLVLLK
CYP2D15	GTTLITNLSSVLK
	VQQEIDEVIGR
	DTEVQGFLIPK
CYP2E1	GEVFAFQSHK
	GITFNNGPGWK
	EIPFLLEALR
CYP3A12	LNAQGIIQPEKPIVLK
CYP3A26	GIIQPEKPVVLK

MRM Q1/Q3 Ion Pair Selection by Syringe-Infusion

Stable isotope peptide standards AQUA Ultimate grade were obtained from Thermo Fisher Scientific GmbH (Ulm, Germany). The stable isotope label (^{13}C, ^{15}N) was incorporated at the lysine or arginine position resulting in a mass shift of +8 Da or +10 Da respectively. Isotopically-labeled peptides were diluted to 100 fmol/μL (100 nM) in 50% (v/v) acetonitrile, 0.1% (v/v) formic acid for infusion, at a flow rate of 20 μL/min using a Harvard syringe pump 11 (Harvard Apparatus, Holliston, MA). Infused peptide standard solutions were analyzed by electrospray using a 4000 QTRAP hybrid triple quadrupole/linear ion trap MS (Applied Biosystems/MDS Sciex) equipped with a turbo ionization source. MS analysis was conducted in the positive ion mode with an ion spray voltage of 5500 V. Collision energy, declustering potential and collision cell exit potential were optimized for maximum transmission and sensitivity of each MRM transition using the Quantification Optimization function provided in Analyst 1.5.

MRM Analysis of Dog Microsomes Digests

Prior to MRM analysis, samples were reconstituted in 3% (v/v) acetonitrile in 0.1% (v/v) formic acid to a concentration of ~1.5 mg/ml based on an initial protein concentration of dog intestinal and liver microsomes.

Before analysis by MRM, 25 μl of heavy stable isotope–labeled internal standard solution (20 fmol/μl of each peptide) was added to 25 μl of sample and 10 μl out of this solution was injected as triplicates.

Analysis was carried out in scheduled MRM mode with a MRM detection window of 48 s and a target scan time of 1 s enabling sufficient points across a peak for accurate quantitation. Typical instrument settings included a spray voltage of 5.5 kV, an ion source temperature of 500°C, a GS1 (nebulizer gas) setting of 40, a GS2 (auxiliary gas) setting of 40, a curtain gas setting of 25 and a CAD pressure at 4.7×10^{-5} Torr. A minimum of three transitions per peptide were monitored for each light and heavy peptide and acquired at unit resolution both in the first and third quadrupoles (Q1 and Q3) to achieve maximum selectivity and sensitivity in the MRM assay. In general, transitions were chosen based upon relative abundance and m/z greater than the precursor m/z in the full-scan MS/MS spectrum recorded on the 4000 Q Trap mass spectrometer. The final MRM method included 120 optimized MRMs for seven target proteins.

MRM Data Analysis

All MRM data was processed using MultiQuant 1.2 (Applied Biosystems) with Scheduled MRM Algorithm support for peak integration. Peak integrations were reviewed manually and transitions from endogenous peptides were confirmed by the same retention times of the synthetic heavy stable isotope-labeled peptides. The default MultiQuant values for Gaussian smooth width, retention time half window, noise percentage, baseline subtraction window and peak splitting factor were used.

The following biophysical consideration guided the formulation of a statistical model to summarize from transition intensities to protein abundances: After trypsination, a peptide's concentration (Eq. 3, detailed term definitions in Supplementary Material) should be a function of the originating proteins concentration multiplied by a peptide-specific trypsination efficiency factor $f_{Tryps,\ p}$:

$$c(\text{Peptide}) = c(\text{Protein}) * f_{Tryps,\ p} * \varepsilon_1 \tag{3}$$

The number of ionized peptide molecules after Electron Spray Ionization (Eq. 4) is a function of the respective peptide molecule concentration and a peptide specific ionization factor, $f_{Ion,\ p}$:

$$n(\text{Peptide}) = c(\text{Peptide}) * f_{Ion,\ p} * \varepsilon_2 \tag{4}$$

The peak area (PA) of transitions for a given peptide over MS/MS and fragmentation (Eq. 5) is a function of the number of electrospray ionized peptides passing the mass selection in MS and the fragmentation factor, f_{frag}.:

$$PA(\text{transition}) = n(\text{Peptide}) * f_{frag,\ p} * \varepsilon_3 \tag{5}$$

Combining the Eqs. 3 to 5 forms a relation between PA (transition) and protein abundance c(Protein) in a sample (Eq. 6):

$$PA(\text{transition}) = c(\text{Protein}) * f_{Tryps,\ p} * f_{Ion,\ p} * f_{frag}\varepsilon * \tag{6}$$

After log-transformation, factors become addends (Eq. 7):

$$\begin{aligned} \log(PA(\text{transition})) = {} & \log(c(\text{Protein})) \\ & + \log\left(f_{Tryps,\ p} * f_{Ion,\ p}\right) \\ & + \log\left(f_{frag}\right) + \log(\varepsilon *) \end{aligned} \tag{7}$$

This equation can be translated into a linear combination of the effects, where the variable PeptideEffect summarizes the trypsination effect $f_{Tryps,\ p}$ and ionization effect $f_{Ion,\ p}$ for a given peptide; FragmentationEffect is the fragmentation efficiency of the ionized peptide into transition states, f_{frag}. By modeling the PeptideEffect and FragmentationtationEffect using the experimentally determined peak area of the

transitions, the ProteinEffect is an estimate of the protein abundance c(Protein) in a given sample:

$$\log(\mathrm{PA}(\mathrm{transition})) = \mathrm{ProteinEffect} + \mathrm{PeptideEffect} + \mathrm{FragmentationEffect} + \varepsilon \quad (8)$$

The hierarchical nature of this model is appropriately addressed by a mixed effect model where a transition is nested in a peptide which is nested in a protein (17). This was technically implemented using R 2.10.1 (R Development Core Team, 2009) and the R package lme4 (18): before modeling, a data matrix for each protein quantitation group is generated that has the columns PA, SampleName, PeptideID and TransitionID. It contains a row for each combination of SampleName and PeptideID, TransitionID and the respective, experimentally observed PA. Now a linear mixed effect model is formulated (following the syntax of the statistical language "R"):

$$\mathrm{lmer}(\log(\mathrm{PA}) \sim \mathrm{SampleID} + (1|\mathrm{PeptideID}/\mathrm{TransitionID})) \quad (9)$$

Notice the similarity with Eq. 8: The resulting effect estimates of this model for PeptideID are the PeptideEffect of the given peptides, effect estimates of this model for TransitionID are the FragmentationEffect of the given transitions and the effect estimates of SampleID are the ProteinEffect, as the sample name identity describes the effect of a given abundance of a given protein in a given sample to the PA as we have derived above.

Statistical Analysis

Non-parametric tests, Mann-Whitney's for two groups and Dunn's multiple comparisons for several groups, at significance level of 0.05 were used to compare the abundance of total microsomal protein, CYP enzyme expression and specific CYP enzyme activity between liver and intestinal segments. As positive linear correlation between enzyme activity and expression is expected, the correlation between marker metabolic reactions and CYP enzyme expression was tested using Pearson's linear correlation test and one tailed P-value less than 0.05 was considered as statistically significant. Calculations were done using Prism (Version 5.03, GraphPad Software Inc).

RESULTS

The results are presented mainly as figures in this report. Additionally, the data are available also in numerical form in Supplementary Material.

Microsomal Scaling Factors for Beagle Dog Intestine and Liver

The amount of total microsomal protein per mass of whole tissue was lower in the intestine than in the liver (Fig. 1a). However, the amount of total microsomal protein per mass of metabolizing cells was virtually the same in the liver (geometric mean 51 mg/g of liver) and all small intestinal segments (geometric mean 50 mg/g of pelleted enterocytes). For the large intestine, the amount of total microsomal protein in the cecum (geometric mean 13 mg/g of enterocytes) and colon (geometric mean 32 mg/g of enterocytes) were lower. However, with this small number of donors (n=4) only the difference from cecum to small intestine reached statistical significance. The mass of enterocytes per length of intestine was lower in the small intestine than the large intestine leading to a virtually constant amount of

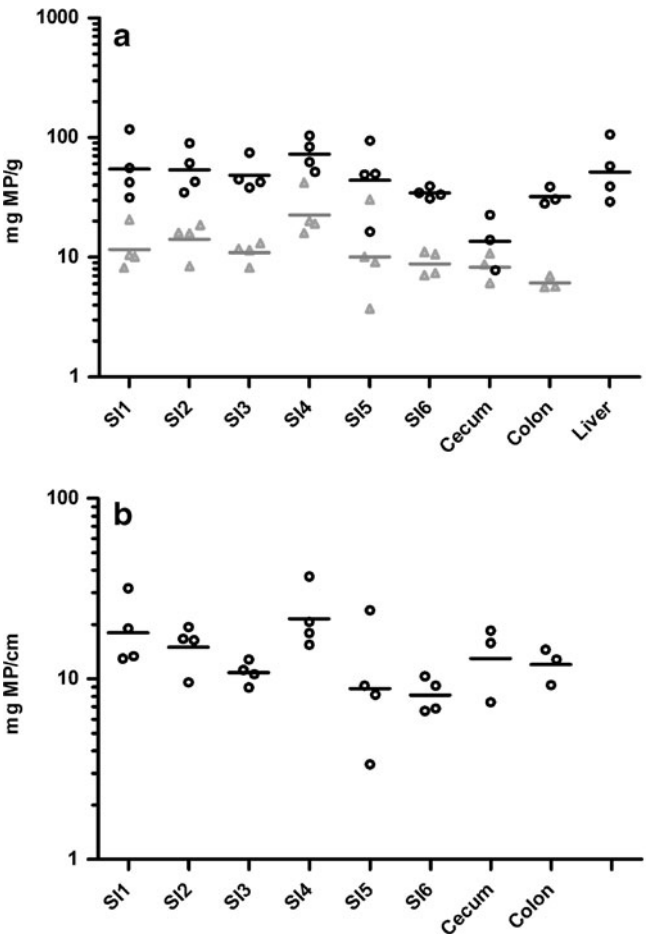

Fig. 1 Abundance of total microsomal protein (MP) in the beagle dog intestine and liver. (**a**) Microsomal protein per mass of intact tissue (*grey triangles*) and per mass of enterocytes/hepatocytes (*black circles*) with approximation that liver consists solely of hepatocytes. (**b**) Microsomal protein per length of intestine. Individual symbols and horizontal lines represent the individual measurements and the geometric mean of four donors, respectively.

microsomal protein per length of intestine, 13 mg/cm (geometric mean, 95% CI=11–15) (Fig. 1b).

CYP Enzyme Abundance and Activity in the Liver and Intestinal Microsomes

Expression of 7 CYP isoenzymes in the liver microsomes were quantified using MRM mass spectrometry based assay (Fig. 2). Geometric mean abundance of individual CYPs was 48 (1A2), 54 (2B11), 35 (2 C21), 53 (2D15), 52 (2E1) 88 (3A12) and 2 (3A26) pmol/mg microsomal protein. Summed together these MRM quantified CYP enzymes correspond to 51 to 92% of spectrally determined total P450 content of the corresponding batch of DLM (data in Supplementary Material). The spectrally determined total P450 content in DIM was below the limit of quantification. All isoenzymes showed substantial variability between DLM batches from individual dogs and all had similar geometric mean expression with only the difference between CYP3A12 and CYP3A26 expression reaching statistical significance.

Two CYP enzymes, CYP2B11 and CYP3A12, were quantifiable in lower quantities in the intestinal microsomes although the expression of both decreased to below the limit of quantification in the distal intestine (Fig. 3a). Similarly, the formation rates of nordiazepam and temazepam, diazepam metabolites formed mainly by CYP2B11 and CYP3A12, respectively (13), were higher in the liver than in intestine and declined slightly from small intestine to colon (Fig. 3b). However, when looking at the correlation of metabolism activity and enzyme expression in individual batches of microsomes, the activity and expression of CYP2B11 in DIM did not show a clear correlation (Fig. 4a). There was a statistically significant correlation between temazepam formation rate and CYP3A12 abundance in DIM (Fig. 4b). The number of

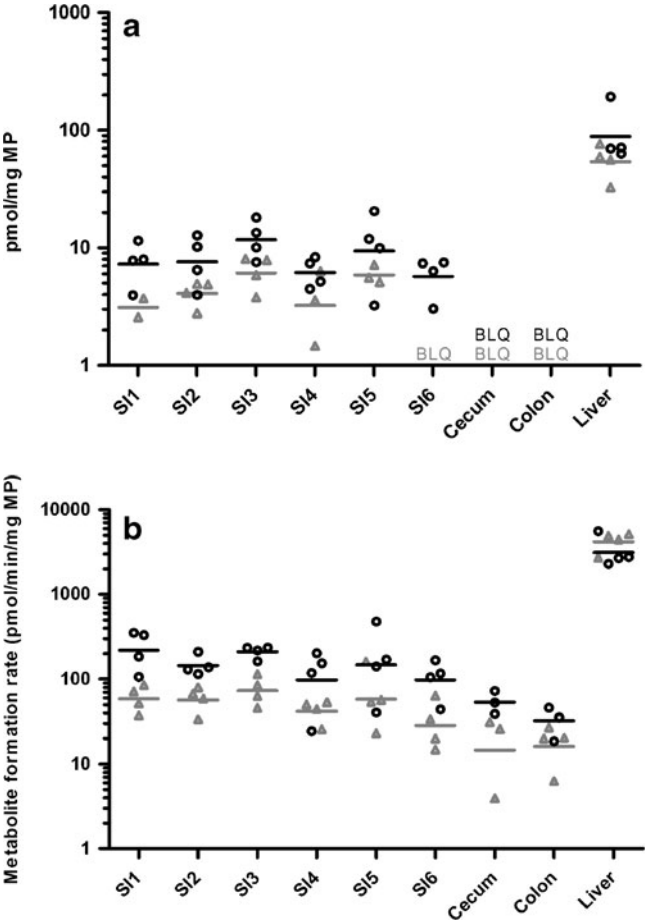

Fig. 3 Abundance (**a**) and activity (**b**) of CYP2B11 (*grey triangles*) and CYP3A12 (*black circles*) in the beagle dog intestine and liver microsomes. The expression of both enzymes declined to below the limit of quantification (BLQ) in the distal part of the intestine. Formation rates of nordiazepam and temazepam in microsomal incubations of 350 μM diazepam were used as the markers of CYP2B11 and CYP3A12 activity, respectively. Individual symbols and horizontal lines represent the individual measurements and the geometric mean of four donors, respectively.

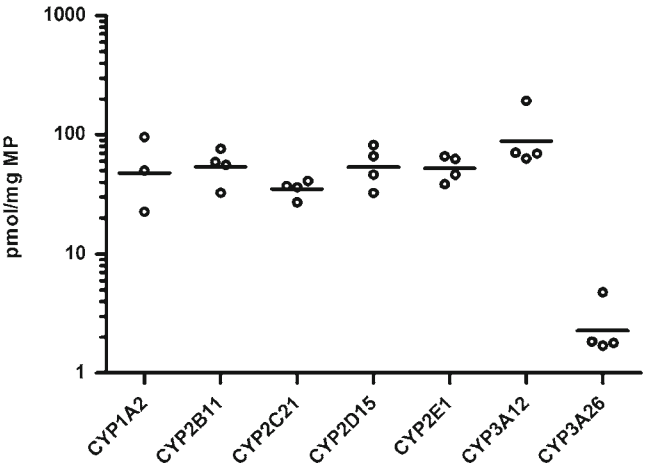

Fig. 2 CYP enzymes expression in the beagle dog liver microsomes. *Circles* and *horizontal lines* represent the individual measurements and the geometric mean of four donors, respectively.

data points originating from liver samples (n=4) is not sufficient for robust statistical inference, but the data do support the expected trend of positive correlation between activity and expression of both CYP2B11 and CYP3A12 in DLM.

Measurement of both enzyme expression and activity in the same microsomal samples allowed for estimation of specific enzyme activity in these samples (pmol/min/pmol CYP). The estimated specific activity of both CYP2B11 and CYP3A12 was highly variable in the intestinal microsomes, whereas liver microsomes showed substantially less variability. Furthermore, the mean estimated specific activity of CYP2B11 was almost 6 fold lower in the intestinal microsomes than in the liver microsomes (mean±standard deviation nordiazepam formation rates in DIM and DLM were 15±9 and 79±9 pmol/min/pmol CYP2B11, respectively). Also the estimated specific activity of CYP3A12 was slightly, but significantly, lower in DIM than in DLM (mean

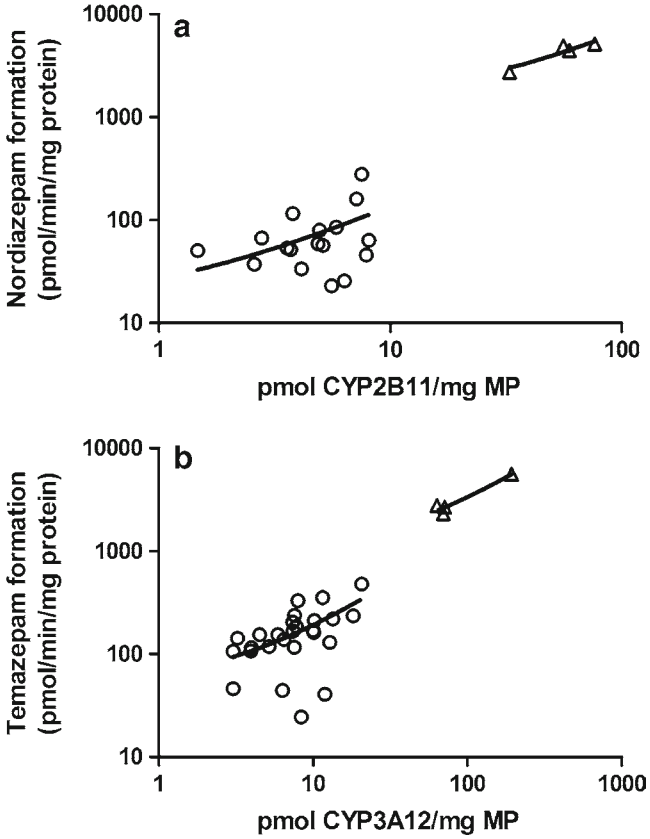

Fig. 4 Metabolite formation rates *vs* expression of CYP2B11 (**a**), and CYP3A12 in DIM (*circles*) and DLM (*triangles*). The solid lines represent the linear regression trend lines, but do not necessarily imply statistically significant correlation (see the text). Formation rates of nordiazepam and temazepam in microsomal incubations of 350 μM diazepam were used as the markers of CYP2B11 and CYP3A12 activity, respectively.

temazepam formation rates in DIM and DLM were 22±11 and 36±6 pmol/min/pmol CYP3A12, respectively).

DISCUSSION

When using PBPK models for human PK predictions and interspecies translation of PK, verification and refinement of models with *in vivo* data in pre-clinical species increases confidence on the appropriateness of PBPK model assumptions (1,19). Therefore, PBPK based prospective predictions of human pharmacokinetics benefit from tools quantifying the significant mechanisms involved in PK for both pre-clinical species as well as human. However, there is a lack of *in vitro/in vivo* scaling factors for intestinal metabolism in pre-clinical species limiting the utility of the pre-clinical verification step in PBPK based predictions of oral PK for intestinally metabolized compounds (19,20). Beagle dogs are often used for preclinical safety testing, clinical formulation development and exploring the potential for food effects. Consequently, this study aimed to establish the enzyme abundance in the beagle dog intestine and liver and to provide missing *in vitro/in vivo* scaling factors for incorporating intestinal metabolism into beagle dog PBPK models. Male and female dogs ranging in age 6–13 months and in weight 6–13 kg were used in the study. The literature data on CYP enzyme expression do not indicate significant gender differences in CYP expression in dogs (21,22) whereas possible impact of age on CYP enzyme abundance in the dog is unknown. The small sample size (n=4) does not allow conclusions on possible impacts of covariates on measured characteristics. However, the data from individual donors is disclosed in the Supplementary Material and, thus, can be compiled with possible follow up studies to explore age dependency of CYP expression.

The main purpose of determination of abundance of total microsomal protein in both intestine and liver was to enable estimation of abundance of individual CYP enzymes in intact tissues after LCMS based quantification of CYP enzymes in microsomes. Estimates of total microsomal protein abundance in liver have been reported for several species, including rat, dog and human (12,23). The amount of total microsomal protein in dog liver (reported values ranging from 43 to 55 mg/g) is approximately the same as that in rat liver (reported values ranging from 35 to 61 mg/g) (23), whereas the estimates for human liver (increasing from ~25 to ~40 mg/g during the first 25 years of life and decreasing slowly thereafter) (24) tend to be slightly lower than for dog and rat. The amount of microsomal protein in the dog liver observed in this study (geometric mean 51 mg/g) is in concordance with the other values reported for the dog, 55 mg/g n=9 (23), 43 mg/g n=1 (25), providing further confidence in the appropriateness of using testosterone-6β-hydroxylation and 7-HC-glucuronidation as microsomal markers instead of some more often applied markers, such as total P450 content.

The use of MRM based quantification of protein is preferable as this form of quantitative mass spectrometry is highly selective and the use of internal stable isotope mass standards in every sample as an internal calibrator ensures a high level of assay precision. Consequently, several recent studies have also utilized MRM based techniques to quantify enzymes and also transporters both *in vitro* and *in vivo* with the aim to establish abundance based *in vitro/in vivo* scaling factors for metabolism and active transport (26–28). To our knowledge, this is the first study reporting MRM based analysis of dog CYP enzymes, whereas the abundance of various CYP enzymes in dog microsomes has been quantified using immunologically based methods, Western Blotting and ELISA. Abundance of CYP2D15 in DLM has been reported previously (29). Additionally, Nishibe and co-workers quantified CYP1A1/2, 2B11, 2C21 and 3A12 in DLM (21). The same group of investigators quantified CYP3A12 also in DIM (22) showing a similar decreasing trend towards distal intestine as was observed in this study and has been reported for the

expression of CYP3A also in rat and human intestine (10,30). Whereas the ELISA assay used failed to detect the other CYP enzymes in DIM, the enzyme activity studies in the presence and absence of CYP inhibiting antibodies suggested that in addition to CYP3A12, also CYP2B11 might be active in DIM (22). This finding was further corroborated in the current study. The majority of the current results are in line with literature reports (less than 2 fold difference between the geometric mean and the literature references). However, the abundance of CYP2C21 and CYP2D15 reported in the literature is approximately 3 fold higher than that observed in the current study. The reasons for these discrepancies are not known but several can be speculated. One possible reason is true inter-individual (or inter-population) variability in enzyme expression between the studies. All these studies have used only a limited number of donors ($n \leq 10$ or not reported) and, thus, it is possible that the average expression seen in these studies do not reflect the true population average. Another likely reason for discrepancies stems from the differences in the analytical techniques applied. Firstly, whereas the MRM based assay used in the current study is highly selective, there is a higher risk of isoenzyme abundance overestimation when using immunologically based assays due to cross reaction of the antibodies with other CYPs. For instance, one can speculate whether polymorphically expressed CYP2C41 with ~70% amino acid identity to CYP2C21 (31) has contributed to the CYP2C21 expression quantified at a time when CYP2C41 was not yet identified (21). Secondly, reliability of absolute quantification is always dependent upon the reliability and relevance of the concentration standard used. For CYP enzymes quantified with immunologically based assays the concentration standards used are typically either purified enzymes or enzymes in recombinant expression systems. However, the purity of standards used and especially the methods used to establish the nominal concentration of the standard are often not disclosed in detail. Oftentimes, the nominal concentration of the standard is based on spectrally determined total CYP content in a sample containing only one CYP isoenzyme. Thus, the nominal concentration in the standard represents the abundance of holo-protein, i.e. CYP enzyme in its active form containing the heme. In contrast, in immunquantification the signal actually originates from apoprotein, which comprises both holo- and non-holo-proteins. Consequently, differences in holo to apo ratio in microsomal samples and standards may have a significant effect on immunoquantification of CYP enzymes in microsomal samples (32). Also MRM based quantification is unable to distinguish between holo- or non-holo proteins in the sample, i.e. apoprotein is quantified. However, the MRM based approach applied in the current study used heavy-labeled peptides, instead of full proteins, as concentration standards. Consequently, the assay is not biased by differences in holo to apo ratios between standards and samples. On the other hand, a drawback of the current approach is the fact that the recovery of peptides during protein digestion process is not controlled. This is a commonly applied approach in the recent reports of MRM based absolute quantification of metabolic enzymes and transporters (28,33,34). Moreover, the limited data available in the literature providing direct comparison of the absolute abundance quantified by MRM based and immunological methods of membrane bound proteins suggest that the assumption of 100% recovery during protein digestion does not cause a major bias between these quantification methods (28,34) However, underestimation of absolute CYP abundance in this study cannot be ruled out. Consequently, there is a possibility that differences in the recovery of peptides originating from different isoenzymes have affected the comparability of abundance between isoenzymes. Anyhow, the recovery of the digestion process is reproducible and, thus, possible underestimation of absolute quantities does not compromise comparability of the abundance of individual CYPs between different samples.

The estimated specific activity of CYP2B11 and CYP3A12 were significantly lower in DIM than in DLM. This is in contrast with the generally applied assumption that there are no significant differences in CYP activity between human gut wall and liver (35–37). However, as the intestinal contents provide a hostile environment in terms of enzyme stability, it is unclear if the difference in estimated specific enzyme activities reflect a true difference in intact tissues or if this is due to loss of enzyme activity during the preparation of intestinal microsomes. Consequently, it is currently not fully clear if *in vitro/in vivo* scaling of intestinal metabolism should be based on the assumption that specific activity of these enzymes in intestine is equal to that in DIM (applicable to scenario that specific activity observed in DIM reflects the activity in intact tissue) or that in DLM (applicable to scenario that specific activity observed in DIM is reduced due to enzyme instability and the true specific activity in intestine is not significantly different from liver). This open question is currently the subject of further research using PBPK modeling of reference substrates which are subject to intestinal metabolism and will be reported in due course.

CONCLUSION

This study characterized the abundance of major CYP enzymes in the beagle dog intestine and liver and these results can be used as the basis of for *in vitro/in vivo* scaling of intestinal and hepatic metabolism. However, further studies are warranted to validate this expectation and to gain further insight on the utility of the enzyme abundance data for understanding and predicting intestinal metabolism in the beagle dog. Such studies are currently ongoing in our laboratory.

ACKNOWLEDGMENTS & DISCLOSURES

The authors thank Pascal Schenk and Paul Schmid for their contribution in setting up the analytical methods for diazepam metabolites.

REFERENCES

1. Jones HM, Parrott N, Ohlenbusch G, Lave T. Predicting pharmacokinetic food effects using biorelevant solubility media and physiologically based modelling. Clin Pharmacokinet. 2006;45:1213–26.
2. Parrott N, Lukacova V, Fraczkiewicz G, Bolger MB. Predicting pharmacokinetics of drugs using physiologically based modeling–application to food effects. AAPS J. 2009;11:45–53.
3. Thelen K, Dressman JB. Cytochrome P450-mediated metabolism in the human gut wall. J Pharm Pharmacol. 2009;61:541–58.
4. Gertz M, Davis JD, Harrison A, Houston JB, Galetin A. Grapefruit juice-drug interaction studies as a method to assess the extent of intestinal availability: utility and limitations. Curr Drug Metab. 2008;9:785–95.
5. Locuson CW, Ethell BT, Voice M, Lee D, Feenstra KL. Evaluation of Escherichia coli membrane preparations of canine CYP1A1, 2B11, 2C21, 2C41, 2D15, 3A12, and 3A26 with coexpressed canine cytochrome P450 reductase. Drug Metab Dispos. 2009;37:457–61.
6. Fasco MJ, Silkworth JB, Dunbar DA, Kaminsky LS. Rat small intestinal cytochromes P450 probed by warfarin metabolism. Mol Pharmacol. 1993;43:226–33.
7. Zhang QY, Dunbar D, Ostrowska A, Zeisloft S, Yang J, Kaminsky LS. Characterization of human small intestinal cytochromes P-450. Drug Metab Dispos. 1999;27:804–9.
8. Watkins PB. The barrier function of CYP3A4 and P-glycoprotein in the small bowel. Adv Drug Deliv Rev. 1997;27:161–70.
9. Hakooz N, Ito K, Rawden H, Gill H, Lemmers L, Boobis AR, *et al.* Determination of a human hepatic microsomal scaling factor for predicting *in vivo* drug clearance. Pharm Res. 2006;23:533–9.
10. Paine MF, Khalighi M, Fisher JM, Shen DD, Kunze KL, Marsh CL, *et al.* Characterization of interintestinal and intraintestinal variations in human CYP3A-dependent metabolism. J Pharmacol Exp Ther. 1997;283:1552–62.
11. Omura T, Sato R. The carbon monoxide-binding pigment of liver microsomes. I. Evidence for its hemoprotein nature. J Biol Chem. 1964;239:2370–8.
12. Barter ZE, Bayliss MK, Beaune PH, Boobis AR, Carlile DJ, Edwards RJ, *et al.* Scaling factors for the extrapolation of *in vivo* metabolic drug clearance from *in vitro* data: reaching a consensus on values of human microsomal protein and hepatocellularity per gram of liver. Curr Drug Metab. 2007;8:33–45.
13. Shou M, Norcross R, Sandig G, Lu P, Li Y, Lin Y, *et al.* Substrate specificity and kinetic properties of seven heterologously expressed dog cytochromes p450. Drug Metab Dispos. 2003;31:1161–9.
14. Addona TA, Abbatiello SE, Schilling B, Skates SJ, Mani DR, Bunk DM, *et al.* Multi-site assessment of the precision and reproducibility of multiple reaction monitoring-based measurements of proteins in plasma. Nat Biotechnol. 2009;27:633–41.
15. Agger SA, Marney LC, Hoofnagle AN. Simultaneous quantification of apolipoprotein A-I and apolipoprotein B by liquid-chromatography-multiple- reaction-monitoring mass spectrometry. Clin Chem. 2010;56:1804–13.
16. Lange V, Picotti P, Domon B, Aebersold R. Selected reaction monitoring for quantitative proteomics: a tutorial. Mol Syst Biol. 2008;4:222.
17. Xia JQ, Sedransk N, Feng X. Variance component analysis of a multi-site study for the reproducibility of multiple reaction monitoring measurements of peptides in human plasma. PLoS One. 2011;6:e14590.
18. Douglas B, Maechler M. Linear mixed-effects models using S4 classes, *R package version 0999375–35*, 2010.
19. Jones HM, Parrott N, Jorga K, Lave T. A novel strategy for physiologically based predictions of human pharmacokinetics. Clin Pharmacokinet. 2006;45:511–42.
20. Jones HM, Gardner IB, Collard WT, Stanley PJ, Oxley P, Hosea NA, *et al.* Simulation of human intravenous and oral pharmacokinetics of 21 diverse compounds using physiologically based pharmacokinetic modelling. Clin Pharmacokinet. 2011; 50:331–47.
21. Nishibe Y, Wakabayashi M, Harauchi T, Ohno K. Characterization of cytochrome P450 (CYP3A12) induction by rifampicin in dog liver. Xenobiotica. 1998;28:549–57.
22. Kyokawa Y, Nishibe Y, Wakabayashi M, Harauchi T, Maruyama T, Baba T, *et al.* Induction of intestinal cytochrome P450 (CYP3A) by rifampicin in beagle dogs. Chem Biol Interact. 2001;134:291–305.
23. Smith R, Jones RD, Ballard PG, Griffiths HH. Determination of microsome and hepatocyte scaling factors for *in vitro/in vivo* extrapolation in the rat and dog. Xenobiotica. 2008;38:1386–98.
24. Barter ZE, Chowdry JE, Harlow JR, Snawder JE, Lipscomb JC, Rostami-Hodjegan A. Covariation of human microsomal protein per gram of liver with age: absence of influence of operator and sample storage may justify interlaboratory data pooling. Drug Metab Dispos. 2008;36:2405–9.
25. Bäärnhielm C, Dahlbäck H, Skånberg I. *In vivo* pharmacokinetics of felodipine predicted from *in vitro* studies in rat, dog and man. Acta Pharmacol Toxicol (Copenh). 1986;59:113–22.
26. Miliotis T, Ali L, Palm JE, Lundqvist AJ, Ahnoff M, Andersson TB, *et al.* Development of a highly sensitive method using LC-MRM to quantify membrane P-glycoprotein in biological matrices and relationship to transport function. Drug Metab Dispos. 2011;39:2440–9.
27. Uchida Y, Ohtsuki S, Kamiie J, Terasaki T. Blood-Brain Barrier (BBB) Pharmacoproteomics (PPx): Reconstruction of *in vivo* brain distribution of 11 P-glycoprotein substrates based on the BBB transporter protein concentration, *in vitro* intrinsic transport activity, and unbound fraction in plasma and brain in mice. J Pharmacol Exp Ther. 2011.
28. Kawakami H, Ohtsuki S, Kamiie J, Suzuki T, Abe T, Terasaki T. Simultaneous absolute quantification of 11 cytochrome P450 isoforms in human liver microsomes by liquid chromatography tandem mass spectrometry with in silico target peptide selection. J Pharm Sci. 2010;100:341–52.
29. Sakamoto K, Kirita S, Baba T, Nakamura Y, Yamazoe Y, Kato R, *et al.* A new cytochrome P450 form belonging to the CYP2D in dog liver microsomes: purification, cDNA cloning, and enzyme characterization. Arch Biochem Biophys. 1995;319:372–82.
30. Mitschke D, Reichel A, Fricker G, Moenning U. Characterization of cytochrome P450 protein expression along the entire length of the intestine of male and female rats. Drug Metab Dispos. 2008; 36:1039–45.
31. Blaisdell J, Goldstein JA, Bai SA. Isolation of a new canine cytochrome P450 CDNA from the cytochrome P450 2C subfamily (CYP2C41) and evidence for polymorphic differences in its expression. Drug Metab Dispos. 1998;26:278–83.
32. Perrett HF, Barter ZE, Jones BC, Yamazaki H, Tucker GT, Rostami-Hodjegan A. Disparity in holoprotein/apoprotein ratios of different standards used for immunoquantification of

hepatic cytochrome P450 enzymes. Drug Metab Dispos. 2007; 35:1733–6.
33. Achour B, Barber J, Rostami-Hodjegan A. Cytochrome P450 Pig Liver Pie: Determination of individual cytochrome P450 isoenzyme contents in microsomes from two pig livers using LC MS. Drug Metab Dispos. 2011.
34. Kamiie J, Ohtsuki S, Iwase R, Ohmine K, Katsukura Y, Yanai K, *et al.* Quantitative atlas of membrane transporter proteins: development and application of a highly sensitive simultaneous LC/MS/MS method combined with novel in-silico peptide selection criteria. Pharm Res. 2008;25:1469–83.
35. Galetin A, Houston JB. Intestinal and hepatic metabolic activity of five cytochrome P450 enzymes: impact on prediction of first-pass metabolism. J Pharmacol Exp Ther. 2006;318:1220–9.
36. Gertz M, Harrison A, Houston JB, Galetin A. Prediction of human intestinal first-pass metabolism of 25 CYP3A substrates from *in vitro* clearance and permeability data. Drug Metab Dispos. 2010;38:1147–58.
37. Yang J, Tucker GT, Rostami-Hodjegan A. Cytochrome P450 3A expression and activity in the human small intestine. Clin Pharmacol Ther. 2004;76:391.